Wave run-up prediction and observation in a micro-tidal beach

Diana Di Luccio[1], Guido Benassai[2], Giorgio Budillon[1], Luigi Mucerino[3], Raffaele Montella[1], and Eugenio Pugliese Carratelli[4]

[1]University of Naples "Parthenope", Science and Technologies Department, Centro Direzionale Is. C4, 80143 Napoli, Italy
[2]University of Naples "Parthenope", Engineering Department, Centro Direzionale Is. C4, 80143 Napoli, Italy
[3]University of Genova, Department of Earth, Environment and Life Sciences, Corso Europa 26, 16132 Genova, Italy
[4]Inter-University Consortium for the Prediction and Prevention of Major Risks Hazards (CUGRI), 84080 Penta di Fisciano (SA), Italy

Correspondence to: Diana Di Luccio (diana.diluccio@uniparthenope.it)

Abstract. Extreme weather events have significant impacts on coastal human activities and related economy. In this scenario, the forecast of sea storms and wave run-up events, in order to mitigate the effects of waves on shores, piers and coastal structures, is a challenging goal. To this end, we used a computational model chain based on both community and ad-hoc developed numerical calculator to evaluate the beach inundation levels, and compared the results of simulated and observed wave run-up levels on a micro-tidal beach located on the northern Tyrrhenian Sea. The offshore wave simulations were performed by a version of WaveWatch III model, implemented by Campania Center for Marine and Atmospheric Monitoring and Modelling (CCMMMA) - University of Naples "Parthenope", which were used as initial conditions for run-up calculations using different empirical formulas. The validation of the simulated wave characteristics was performed using different observation systems, remote sensing data for offshore waves and observations taken from a video camera system for the run-up levels. The usual statistical errors were taken as a measurement of the capability of the modelling system to properly simulate the beach run-up during a storm.

The run-up $Ru_{2\%}$ formulas were classified in terms of their agreement with the observed values. The best agreement was obtained by the Holman (1986) formula (RMSE=0.40), followed by the Mase (1989) equation (RMSE=0.70) and by the Stockdon et al. (2006) equation (RMSE=0.95).

The results of this validation study suggest that the empirical run-up formulas, used in coastal vulnerability context, have to be managed with caution, particularly on gravel beaches.

Keywords: model chain, wave numerical model, beach run-up, video monitoring.

1 Introduction

The monitoring and the forecasting of wind wave interaction processes become particularly critical along the coastal areas, which are highly dynamic complex systems that respond in a nonlinear manner to external perturbations, giving rise to coastal vulnerability (Didenkulova, 2010; Di Paola et al., 2014), and coastal risk due to sea level rise (Benassai et al., 2015a) and subsidence (Aucelli et al., 2016). The main damage caused by extreme wave events is due to sea waves hitting coastal structures, such as bathing facilities still on the beach during the winter season (Casella et al., 2014). Based on these premises, the

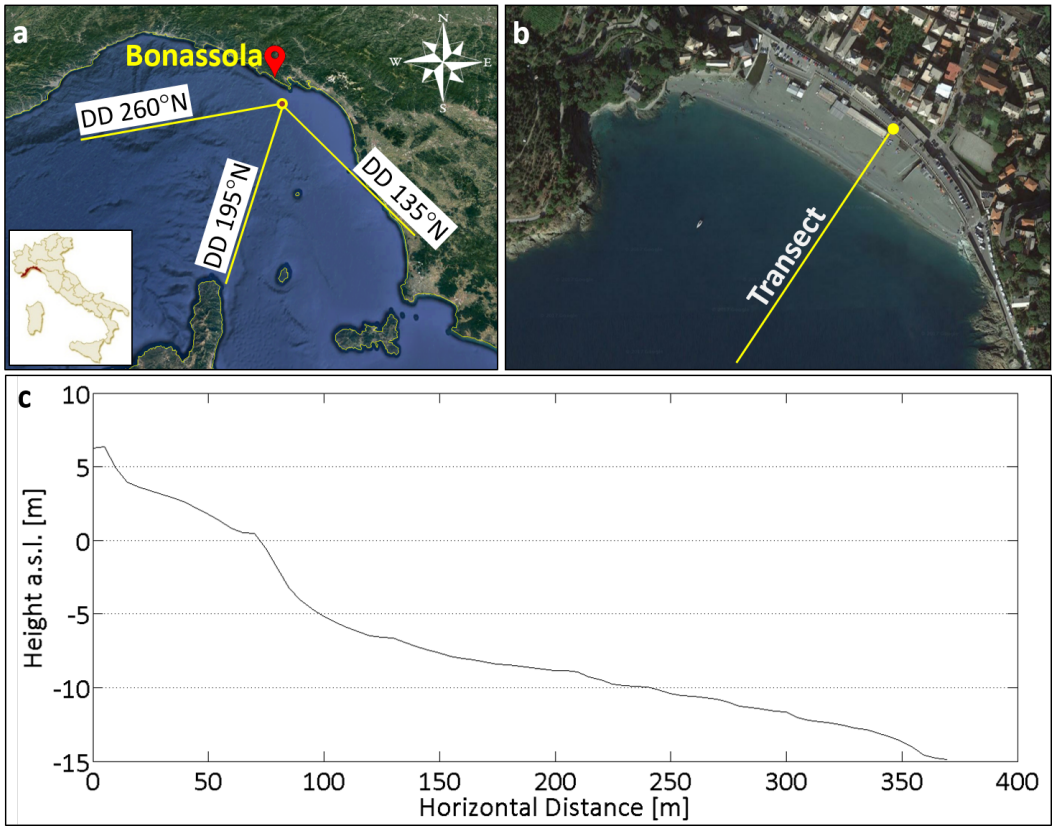

Figure 1. Bonassola beach study area with (a) main and secondary fetches; (b) the monitored transect with video-camera location (yellow circle); (c) the beach profile along the transect.

evolution of winds, waves and the wind-driven sea circulation is of great applicative relevance for both the modelling and the forecasting of the wave climate (Bertotti and Cavaleri, 2009; Cavaleri and Rizzoli, 1981; Mentaschi et al., 2013; Benassai and Ascione, 2006a) and the observation of oceanographic phenomena (Bidlot et al., 2002). The wind wave simulations critically depend on the quality of the driving wind fields (Rusu et al., 2014), which are provided by forecasting and/or climatological winds or alternatively by active satellite-based microwave Synthetic Aperture Radar (SAR) (Johannessen and Bjorgo, 2000). The comparison between the wave simulations obtained by these different data sources has demonstrated the capability of the SAR-based wind field retrieval to improve coastal wind wave modelling (Benassai et al., 2013a, b, 2015b). In regard to coastal zone monitoring, the coastal evolution can be surveyed by remote sensing acquisition (Nunziata et al., 2016), while shorter time scale beach processes can be observed by UAV (Benassai et al., 2017) and video monitoring (Brignone et al., 2012).

In particular, wave run-up prediction is required in most coastal vulnerability and risk evaluation projects (Didenkulova and Pelinovsky, 2008; Didenkulova et al., 2010). Although a number of available numerical models (Dodd, 1998; Hubbard and Dodd, 2002) give accurate estimates of wave run-up for given boundary conditions, simplified run-up formulas are useful to give realistic results on existing cross-shore profiles. The earliest formulation of run-up height was provided in Hunt (1959)

who calculated run-up from incident regular waves. Later research included irregular waves and statistical values of the obtained run-up levels, that is Ru_{max} (the highest run-up height during each run), $Ru_{2\%}$ (the 2% excess run-up height), $Ru_{10\%}$ (the average of the highest one-tenth of the total run-up heights), $Ru_{33\%}$ (the one-thirds of the highest run-up heights), Ru_{mean} (the average of the total run-up heights). Mase (1989) introduced two coefficients which are dependent on the characteristic run-up level $Ru_{x\%}$, as defined in section 3.2. Stockdon et al. (2006) considered the run-up level $Ru_{2\%}$ as a function of the two different contributions of wave set-up and swash.

In this paper we compute the wave run-up levels with the previous different formulations to obtain run-up time series. Since no local measurements from buoys were available (Montella et al., 2008), a version of WaveWatch III (WW3) model implemented by Campania Center for Marine and Atmospheric Monitoring and Modelling (CCMMMA) - University of Naples "Parthenope", was used, taking full benefits of a high spatial resolution weather-ocean forecasting system with a high performance computing (HPC) system for simulation and open environmental data dissemination (Montella et al., 2007). This deep-water numerical model (Ascione et al., 2006) was coupled with a wave propagation model in shallow water which provided the run-up evaluation on the beach. This model chain was tested on a micro-tidal beach located on the northern Tyrrhenian Sea, in order to assess the reliability of the wave modelling system, already verified beforehandin offshore conditions by means of in situ and remote sensing techniques (Carratelli et al., 2007; Reale et al., 2014; Benassai and Ascione, 2006b) also for the simulation of the beach processes. For this purpose, offshore wave simulations, associated with a typical one-year return period storm were previously validated with remote sensing data (as carried out by (Montuori et al., 2011; Benassai et al., 2012)) and then used to initial conditions for run-up calculations using different formulas, which were were validated with observations by camera system using timestack images. The whole procedure demonstrated the capability of the modelling system to properly simulate the beach inundation levels, and its consequent reliability to be used in coastal vulnerability and risk studies.

Innovation: Although, in recent years a number of papers have been published on the offshore validation of numerical simulation models, as well as on the nearshore validation of run-up formulas, to the best of our knowledge, very few studies on a global verification of an operational model chain which starts from the forecasted wind till wave and run-up calculation on the beach, have been published

This paper is organized as follows: the field data and the numerical models and the field data are reported in chapter 2 and 3, the results and the comparison with field data are given in chapters 4. Last, the discussion and the conclusion are reported in chapter 5 and 6, respectively.

2 Study area and wave climate

The test case presented in this paper was carried out on Bonassola beach (La Spezia, Italy), approx. 410m long, which is located on the eastern coast of Liguria. The coastline is oriented South-East/North-West, so although it is exposed to waves coming from South-West (215°-245°), while it is protected by the South-East waves. According to Jennings and Shulmeister (2002), Bonassola beach can be classified as MSG beach due to its sediment characteristics and its morphology. The range of mean sediment grain size in the swash zone is 0.76mm to 62.65mm (0.38 to -5.96 ϕ). The mean beach slope is approximately 8.3%

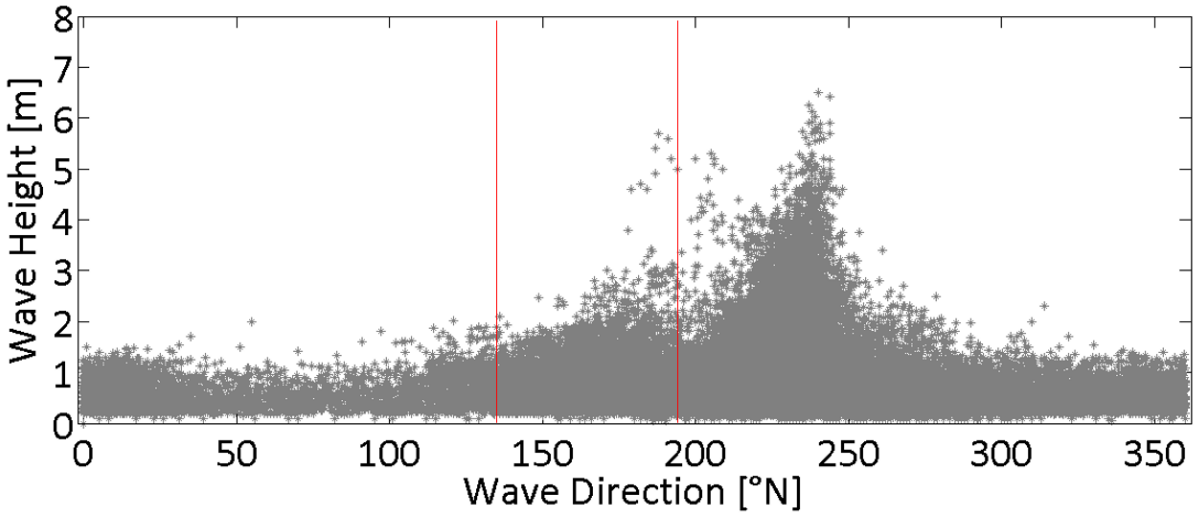

Figure 2. Significant wave heights and wave directions recorded from the SWAN buoy of La Spezia 1989-2009.

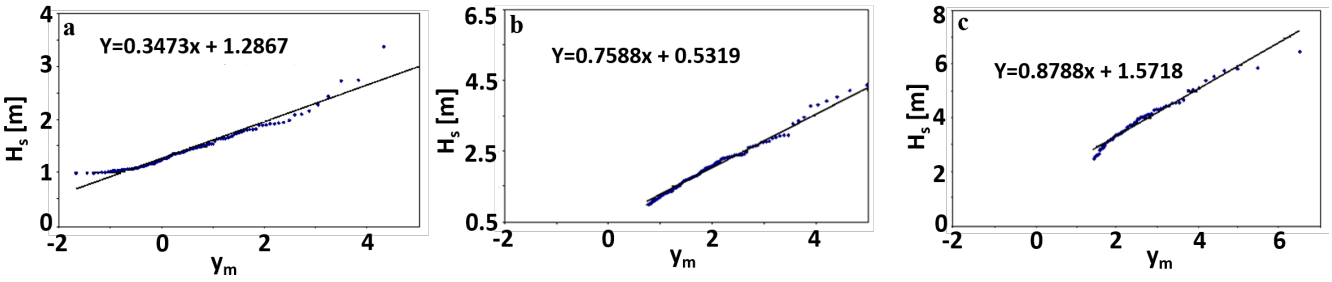

Figure 3. Matching between the recorded extreme wave heights and the reduced variable for Gumbel distribution function for waves coming from a) 135°N-195°N; b) 195°N-225°N; c) 225°N-260°N.

from the shoreline to 10m water depth and becomes 5.5% between 10m and 30m (Fig. 1c). The offshore beach is composed by mean and coarse sand.

Directions 195°N and 260°N limit the main fetch, while the directions 135°N and 195°N limit the secondary fetch (in the following S_1).

In order to analyze the extreme sea events, the offshore wave climate was extracted using the data recorded by Italian SWAN (Sea WAve measurement Network) buoy located offshore La Spezia (43°55'41.99"N 09°49'36.01"E) since year 1989 till 2009. The main transverse sector was later subdivided into two sub-sectors, 195-225°N (S_2) and 225-260°N (S_3), in which two different wave conditions: maximum H_s lower than 5.5m between 195°N and 225°N and higher than 5.5m between 225°N and 260°N (Fig. 2). The H_s time series was processed to obtain the extreme sea storm events. In order to obtain a statistically significant time series, a representative sample of statistically independent extreme wave events N was selected on the basis of

the Peak Over Threshold method (Goda, 1989). The 48h-maxima based on over-threshold H^* time series has been sorted in order to find the best fit between the data and the Gumbel (Fisher-Tippet I) cumulative probability distribution function.

$$P(H) = e^{-e^{-\left(\frac{H-B}{A}\right)}} \tag{1}$$

where A is the location parameter and B is the scale parameter. A rank index m, ranging from 1 to N was associated to order the array and the sample rate of non-exceedance $F(H_s<H^*)$ was calculated as

$$F(H_s) < H^* = 1 - \frac{m - 0.44}{N + 0.12} \tag{2}$$

and it is assumed coincident with the non exceedance probability.

$$y_m = -ln[-lnF(H_s < H^*)] \tag{3}$$

Figure 3 shows the rate between $H_s<H^*$ and relative reduced variable for waves coming from each directional sector.

The linear regression line y=ax+b is given as

$$H_s = Ay_m + B \tag{4}$$

where A (slope of the regression line) and B (line intercept) coefficients are linked with the probability distribution function. The wave heights for different return periods can be determined by the following expressions:

$$H_r = Ay_r + B \tag{5}$$

where H_r is the significant wave height with return period T_r and the relative reduced variable is

$$y_r = -ln\left[-ln\left(1 - \frac{1}{\lambda T_r}\right)\right] \tag{6}$$

and the sample intensity λ is defined by the ratio between the number of extreme events and the number of years of observation. Table 1 gives the offshore wave heights obtained for each directional sector as functions of the relative return period T_r, which are maximum for the western directions (sector S_3), with $H_s>5.0$m.

In order to evaluate the wave run-up levels associated with frequent wave conditions, we chose a recent wave storm coming from a western direction with significant wave heights that can occur several times a year (that is with a return period less than a year). We performed numerical simulations on this storm using the WW3 model accomplished with run-up calculations using different empirical formulas.

3 Methods

3.1 Wave numerical simulations

The weather/sea forecasting tool in Fig. 4, implemented by CCMMMA hosted by the University of Naples "Parthenope", was configured using an HPC infrastructure to manage and run a modeling system based on the algorithms implemented in the

Table 1. Design waves obtained from La Spezia buoy (1989-2009) for different return periods and each directional sector.

T_r	Sector	H_r	y_r	T_r	Sector	H_r	y_r
	S_1	2.84	4.46		S_1	3.88	7.46
1	S_2	3.72	4.20	20	S_2	6.00	7.21
	S_3	5.59	4.57		S_3	8.23	7.57
	S_1	3.40	6.08		S_1	4.20	8.38
5	S_2	4.95	5.82	50	S_2	6.70	8.12
	S_3	7.01	6.19		S_3	9.03	8.49
	S_1	3.64	6.77		S_1	4.44	9.07
10	S_2	5.74	6.51	100	S_2	7.22	8.82
	S_3	7.62	6.88		S_3	9.4	9.18

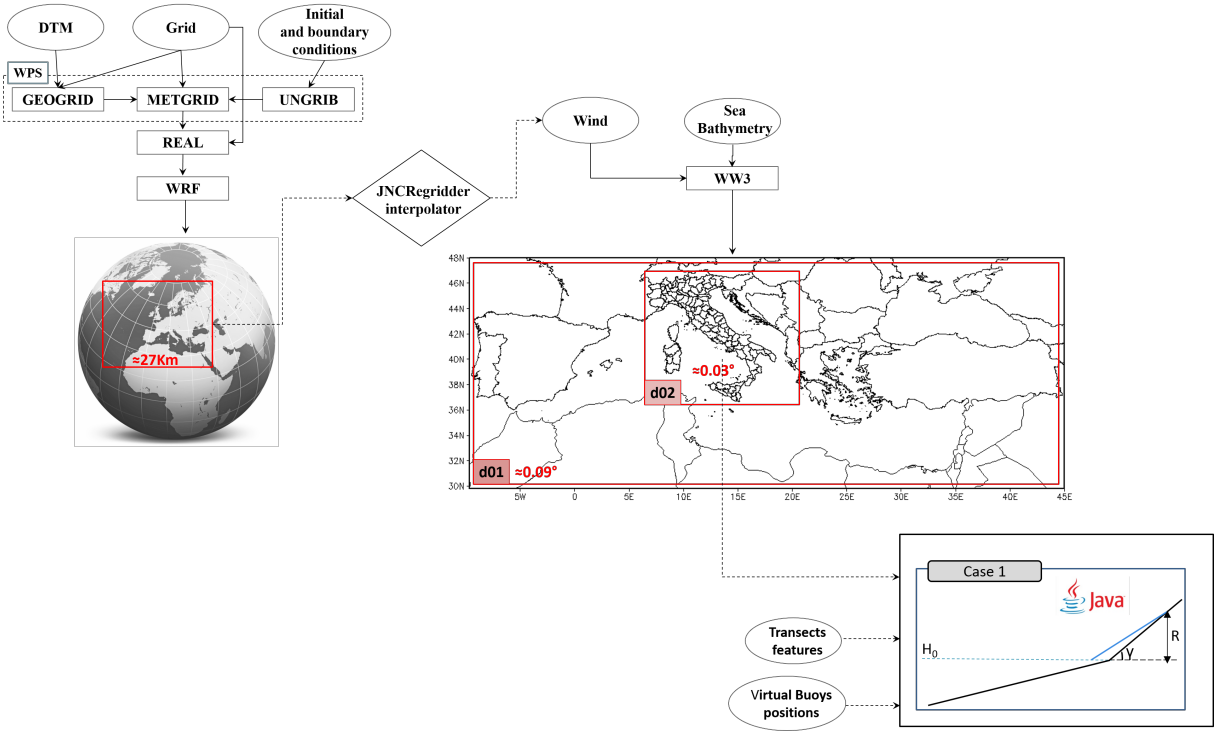

Figure 4. Model chain with the input/output data flux in the model coupling. The case 1 is the implemented run-up model calculator.

open-source numerical models Weather Research and Forecasting (WRF) (Skamarock et al., 2001) and WavewatchIII (WW3) (Tolman et al., 2009) organized in a workflow.

The present operational system is based on complex data acquisition, processing, simulation, post-processing and inter-comparison dataflow, provided by FACE-IT workflow engine (Pham et al., 2012), available as open source and cloud service. This integrated data processing and simulation framework enables: i) the data ingest from geospatial archives; ii) the data regridding, aggregation, and other processing prior to simulation; iii) the leveraging of the high-performance and cloud computing; iv) the post-processing to produce aggregated yields and ensemble variables needed for statistics and model testing. The main workflow tool is the WRF numerical model which gives the 10m wind fields atmospheric forcing needed to drive the WW3 model to estimate the offshore waves, which is the initial and boundary conditions for the modeling of waves in shallow water and run-up/overtopping calculator software.

Wave simulations were carried out using the WW3 model version 3.14, a third generation wave model developed at NOAA/NCEP. The physics packages used in the our implementation are:

- Linear input parametrization of Cavaleri and Rizzoli (1981) with a filter for low-frequency energy as introduced by Tolman (1992). Source term package of Tolman and Chalikov (1996) have been implemented with stability correction;
- Discrete interaction approximation (DIA) (Hasselmann and Hasselmann, 1985) for non-linear wave-wave interactions;
- ULTIMATE QUICKEST propagation scheme (Leonard, 1979) with averaging technique for Garden Sprinkler alleviation Tolman (2002);
- JONSWAP bottom friction formulation (Hasselmann, 1973) with no bottom scattering and Battjes and Janssen (1978) shallow water depth breaking with a Miche-style limiter.

In order to produce the numerical simulations presented in this paper, we configured the WW3 model with two one way nested computational domains:

- **Coarse domain**: the domain d01 covers almost the whole Mediterranean Sea by a grid of 608x203 points spaced by a 0.09° resolution (Lon_{min}=9.65°W, Lon_{max}=44.98°E; Lat_{min}=29.78°N, Lat_{max}=47.96°N)
- **Fine domain**: the d02 domain covers the seas around the Italian peninsula by a grid of 486x353 points spaced by a 0.03° resolution (Lon_{min}=6.33°N, Lon_{max}=20.88°N; Lat_{min}=36.42°E, Lat_{max}=46.98°E).

Using this configuration we avoided the duty of providing boundary conditions on the south and west boundaries of the d02 domain and considered the d01 as a closed domain forced only by the weather conditions provided by the WRF offline coupling.

Outputs from the model include gridded fields with the associated significant wave height (H_s), wave direction (Dir_{mn}), mean period (T_m) and spectral information. The WW3 grid points close to the coast were used as "virtual buoys" (VB) to compute the wave transformation down to the coast, with the final goal of simulating the run-up parameter on the beaches.

3.2 Wave run-up calculator

Since Hunt (1959), who used regular waves, the wave run-up Ru, defined as the vertical elevation above the still water level, has been expressed as:

$$\frac{Ru}{H_0} = \xi \tag{7}$$

where ξ is the Iribarren number or surf similarity parameter (Battjes, 1975)

$$\xi = \frac{tan\beta}{\sqrt{\frac{H_0}{L_0}}} \tag{8}$$

and β is the beach slope angle, H_0 is the deep water significant wave height and L_0 is the linear theory deep-water wavelength (Airy, 1841)

$$L_0 = \frac{gT^2}{2\pi} \tag{9}$$

where T is the wave period. In detail, H_0 depends on the relation between the VB (C_{VB}=L_{VB}/T_m) and the deep water (C_0=L_0/T_m) (Shore Protection Manual, 1984) wave celerity:

$$H_0 = H_s \frac{C_{VB}}{C_0} \tag{10}$$

In VB the wavelength is equal to L_{VB}=(2π)/k in which k is the wavenumber obtained by the Hunt approximation of the standard dispersion relation (Fenton and McKee, 1990):

$$(kd)^2 = \left(\frac{\sigma^2 d}{g}\right)^2 + \frac{\left(\frac{\sigma^2 d}{g}\right)}{1 + \sum_{n=1}^{\infty} d_n \left(\frac{\sigma^2 d}{g}\right)^n} \tag{11}$$

where d_n are six constant values given by Fenton and McKee (1990), and σ is the wave frequency. The beach slope is dynamically calculated by taking into account the profile for each coastal transect considered. The extent of flooding and the corresponding hazard level depends on the beach slope and the run-up parameter.

Dealing with random waves, $Ru_{2\%}$ is defined as the wave run-up level, measured vertically from the still water line, which is exceed by 2% of the number of incident waves (van der Meer et al., 2016).

Holman (1986) proposed an empirical formula to obtain $Ru_{2\%}$, based on Iribarren number ξ_f constrained with surf zone slope angle.

$$\frac{Ru_{2\%}}{H_0} = 0.83\xi_f + 0.2 \tag{12}$$

Mase (1989) on the basis of laboratory tests obtained by the characteristic run-up level x as a foundation of two empirical coefficients a and b.

$$\frac{Ru_{x\%}}{H_0} = a\xi^b \tag{13}$$

Mase suggested a=1.86 and b=0.71 for $Ru_{2\%}$, a=2.32 and b=0.77 for Ru_{max}, a=1.70 and b=0.71 for $Ru_{10\%}$, a=1.38 and b=0.70 for $Ru_{33\%}$, a=0.88 and b=0.69 to obtain Ru_{mean}.

Stockdon et al. (2006) considered the run-up $Ru_{2\%}$ as a function of the two different contributions of wave setup and swash

$$Ru_{2\%} = 1.1\left(0.35\tan\beta_f\left(H_0L_0\right)^{0.5} + \left[H_0L_0\left(0.563\tan\beta_f^2 + 0.004\right)\right]^{0.5}\right) \quad (14)$$

where the first term in brackets represents wave setup contribution, the $\beta_f{}^2$ stands for swash contribution and the 0.004 stands for infragravity contribution.

In random waves, H_0 is substituted with the spectral wave height $H_{m0}=4(m_0)^{0.5}$, defined as the incident significant wave height in shallow water, where m_0 is the zeroth spectral moment, equal to the water elevation variance.

The equation (14) has been used by a number of researchers to compute coastal inundation and consequently coastal vulnerability and risk (Di Paola et al., 2014; Benassai et al., 2015a). Melby et al. (2012) compared the skill of some different run-up models through some statistical measures and introduced a new statistical skill measure, described in section 3.3.2, which was used to compare different formulations for an extensive dataset. In the following, we compared the skill of different run-up equations through the departure from the observed run-up levels evaluated with video camera records. Among the different empirical formulas used to calculate the wave run-up parameters, the last three selected equations have been adopted to obtain run-up time series. In particular, Holman (1986), Mase (1989) and Stockdon et al. (2006) formulas have been used for the 2% wave run-up levels, while only Mase (1989) equation has been used to calculate the 10%, 33%, mean and max run-up levels.

3.3 Observations of offshore waves and beach run-up

3.3.1 Altimeter and video monitoring

The accuracy of the wave model output in offshore conditions was evaluated against remotely sensed data. The altimeter footprint along the satellite tracks provides a large spatial coverage over the entire region of the Central and Northern Tyrrhenian Sea, which cannot be accomplished by in-situ observations at fixed stations. The altimeter data was obtained from the dataset of the Ocean Surface Topography Mission (OSTM/Jason-2), launched on 20 June 2008.

In this case, we used the Geophysical Data Record (GDR) with spatial resolution of 11.2km (Along) x 5.1km (Across). Fig. 5 shows the considered track of the OSTM/Jason2 satellite.

The beach run-up simulations by means of different equations were validated by means of a video monitoring system placed in the middle of Bonassola beach (Fig. 6a,b,c,d). Video recordings of run-up were made using three video cameras, installed at an elevation of about 13m above Mean Sea Level (MSL), which have allowed a complete coverage of the beach since 19 November 2015 to date. Using the geometric transformation between ground and image coordinates, the light intensity of each pixel in the cross-shore transects was digitized. Vertical run-up elevation time series were extracted from video recordings using the time-stack method (Aagaard and Holm, 1989; Holland and Holman, 1997). This methodology, giving rise to the signal reported in Fig. 6e, is described in the extensive literature on coastal video monitoring (Takewaka and Nakamura, 2001; Ojeda et al., 2008; Zhang and Zhang, 2008). The run-up position at each video sample time (1Hz) was obtained with Beachkeeper

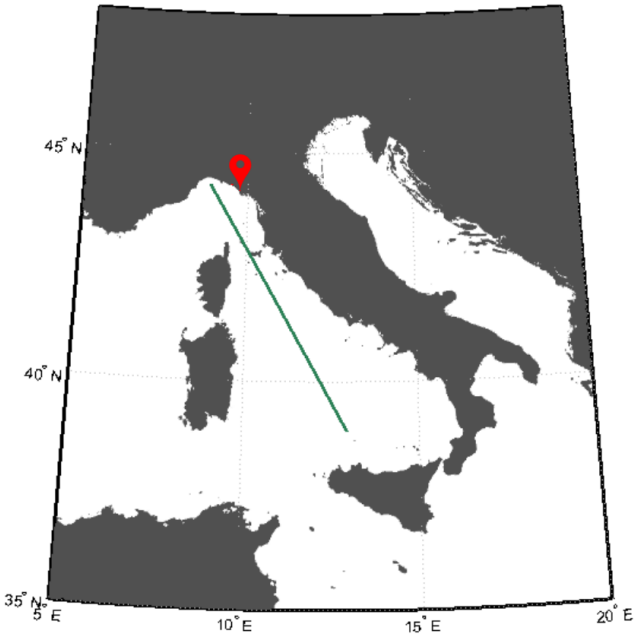

Figure 5. Map showing the position of the dataset to models testing. The green line depicts the OSTM/Jason-2 satellite dataset.

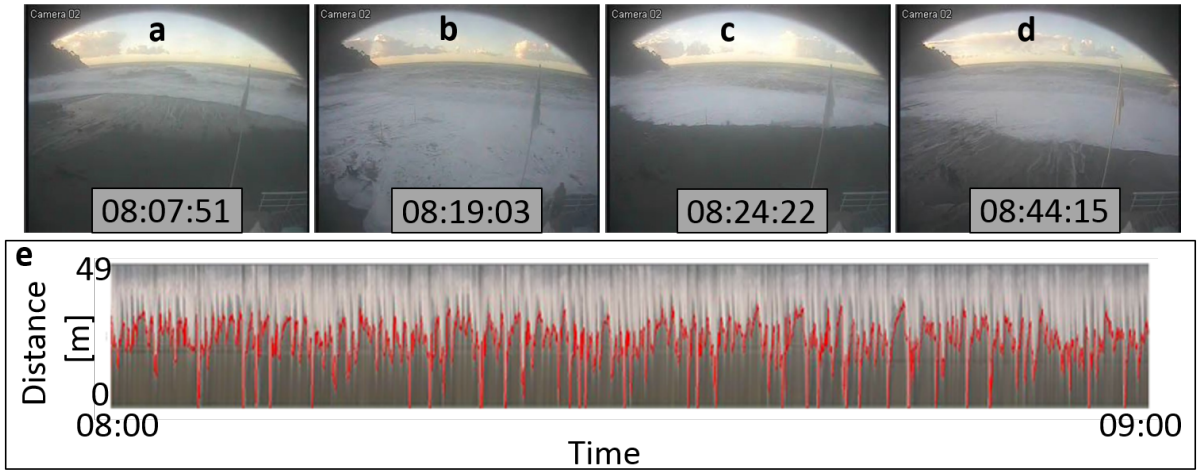

Figure 6. A time sequence (a) (b) (c) (d) of the Bonassola beach sea storm on 10 February 2016; (e) time-stack relative to 10 February 2016 between 08:00-09:00.

plus (Brignone et al., 2012), a software based on Matlab algorithm used to analyze the images without any a-priori information of the acquisition system itself.

3.3.2 Comparison statistics

The quality of the results provided by the offshore wave model and by the run-up simulations was evaluated by the comparison with wave altimeter records and video-camera run-up observations. Deviation of simulated parameters from observed data was estimated through some of the following statistical error indicators (S_i indicate a simulated variable, O_i indicate an observed variable and N is the number of observations):

- normalized Bias (BI):

$$BI = \frac{\sum_{i=1}^{N}(S_i - O_i)}{\sum_{i=1}^{N} O_i} \tag{15}$$

- root mean square error (RMSE):

$$RMSE = \sqrt{\frac{\sum_{i=1}^{N}(S_i - O_i)^2}{N}} \tag{16}$$

- normalized root mean square error (NRMSE):

$$NRMSE = \sqrt{\frac{\sum_{i=1}^{N}(S_i - O_i)^2}{\sum_{i=1}^{N} O_i^2}} \tag{17}$$

- normalized scatter index (SI):

$$SI = \sqrt{\frac{\sum_{i=1}^{N}[(S_i - \bar{S}) - (O_i - \bar{O})]^2}{\sum_{i=1}^{N} O_i^2}} \tag{18}$$

- linear correlation coefficient (R):

$$R = \frac{cov(S_i, O_i)}{var(O_i)var(S_i)} \tag{19}$$

The results are summarized in the Summary Performance Score (SPS) index, based on the RMSE, BI and SI performance, normalized between 0 and 1.

- NRMSE Performance ($NRMSE_P$)

$$NRMSE_P = 1 - NRMSE \tag{20}$$

- BI Performance (BI_P)

$$BI_P = 1 - |BI| \tag{21}$$

– SI Performance (SI_P)

$$SI_P = 1 - SI \tag{22}$$

– Summary Performance Score (SPS)

$$SPS = \frac{NRMSE_P + BI_P + SI_P}{3} \tag{23}$$

4 Experimental results

In this section some meaningful experimental results are presented and discussed to show the capability and accuracy of wind wave modelling chain in estimating run-up levels on the beach studied.

4.1 Offshore wave validation with altimeter data

The consistency of the WW3 model was validated taking full benefit of the ku-based altimeter data from OSTM/Jason2 mission, relative to the passage of the satellite during the period from February 9th 2016 at 04:58:44 UTC to 09th 2016 at 05:00:43 UTC. Figs. 7a,b,c depict the simulated WW3 H_s maps on February 10th 2016 at 00:00, 06:00 and 12:00 UTC, with relative zoom, in Figs. 7d,e,f, respectively, while Fig. 8 shows the time history of the measured and modelled offshore H_s along the track.

The results of the wind-wave modelling system were interpolated in both space and time to collocate with the altimeter data. Firstly, hourly WW3 H_s outputs are first spatially interpolated (bilinear interpolation) from the grid points to the locations of the altimeter measurements. Interpolations are then carried out in time to fit the satellite pass (linear time interpolation between the previous and following field values). The observed H_s is shown as a blue line in Fig. 8a, while the simulated H_s is reported as a red line (the model results are smoother due to minor time resolution). In general, the model fits the measurements quite well, but sometimes underestimates the observations (especially the energy peaks). For example, the first high wave event between 41.5°N and 42°N is underestimated by the model, while the second high wave event between 43.5°N and 44°N is slightly overestimated.

The statistics of the comparison give an R value of 0.838, a BI of 0.192, a SI of 0.202 and a RMSE value of 0.455m. The satisfactory agreement is shown by a RMSE lower than 0.46m and a correlation coefficient higher than 0.83. In fact, Fig. 8 shows a good match between simulations and observations, however non-negligible differences in terms of H_s can be noted. This could be explained by taking into account the different spatial gridding resolution scale of both modeled (WW3) and remotely sensed (Jason-2) wave estimation products.

4.2 Run-up calculation and validation with video-monitoring system

In this subsection, wave run-up numerical simulations accomplished through the operational software calculator using different empirical formulas are described with respect to the storm between February 9th and February 11st 2016. A preliminary offshore wave simulation was performed on a virtual buoy located offshore Bonassola beach. The relative H_s and T_m time history has

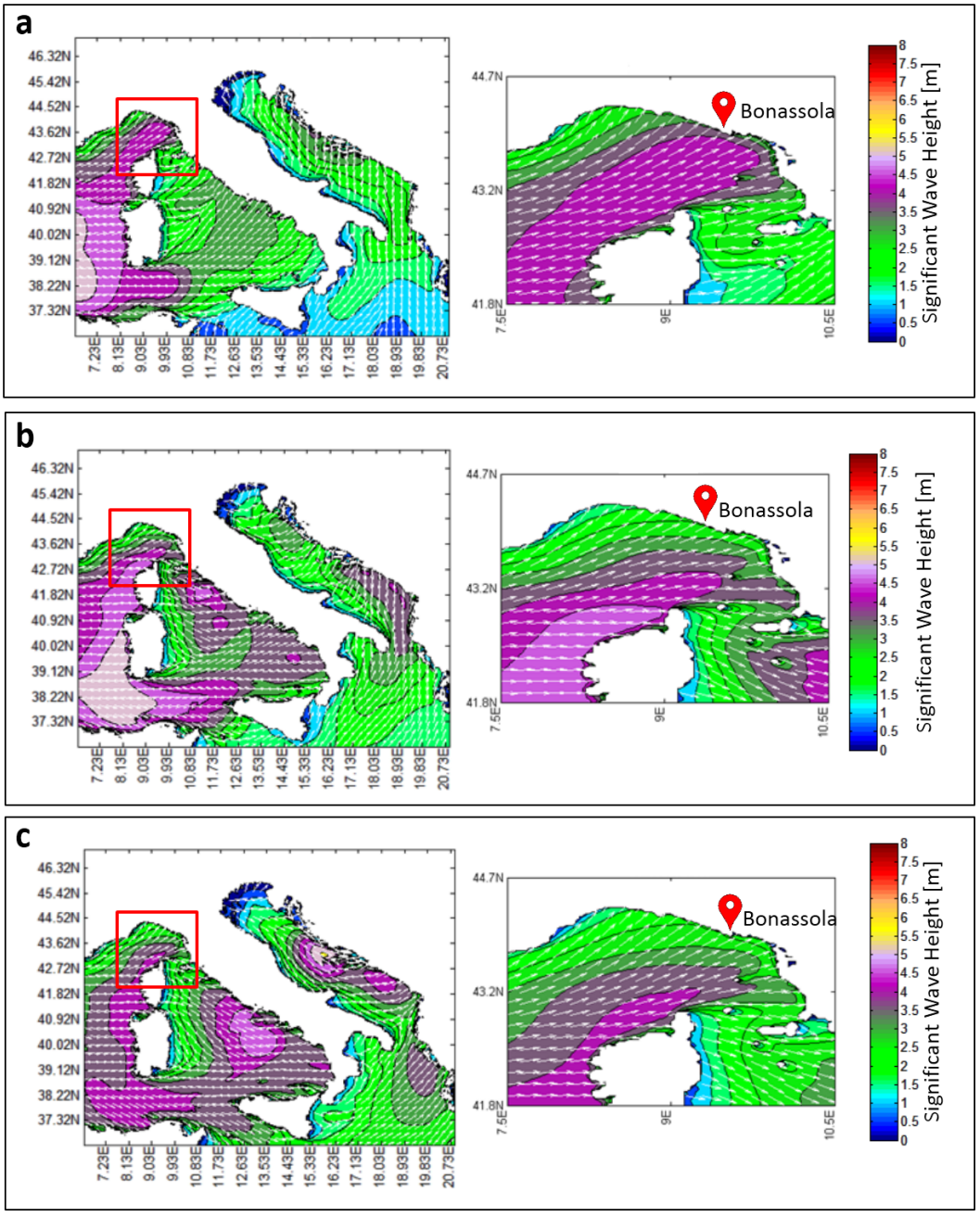

Figure 7. Ligurian Sea significant wave height (color maps) and direction (vector fields) in three moments of sea storm in February 2016. The maps are relative to WW3 model forecast on February 10th 2016 at: (a) 00:00 UTM; (b) 06:00 UTM; (c) 12:00. Wave height isolines are at 0.5m intervals.

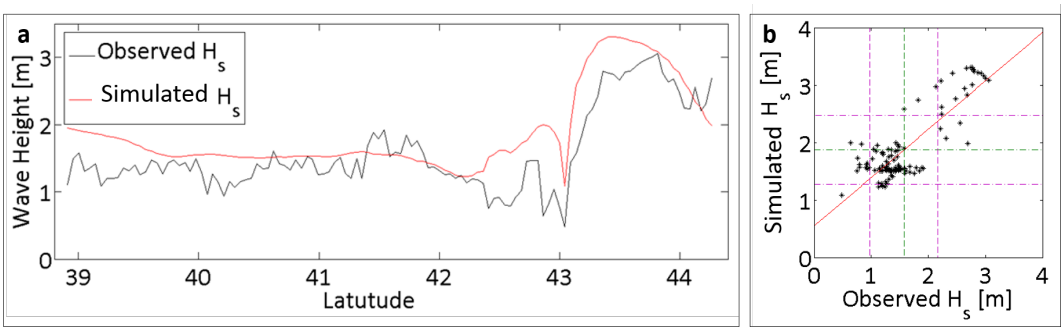

Figure 8. Matching between WW3 and Ku-band altimeter data from JASON-2 satellite pass. 44 cycle 280. (a) Time series during the period from February 9th 2016 at 04:58:44 to 09th 2016 at 05:00:43. (b) Scatter diagram between observed and simulated H_s [m]. The green dotted lines are the mean in x (1.876) and y (1.574) directions, while the purple dotted lines are the relative standard deviation of 0.6022 and 0.5975, respectively.

been reported in Fig. 9a,b, respectively. The storm exhibited a maximum H_s higher than 3.0m on February 10th 2016 at 03:00, followed by a decrease of H_s in the following hours, with values between 2.0m and 3.0m, in accordance with the maps in Fig. 7.

Based on the run-up formulas described in section 3.3 on the transect described in section 2, the run-up levels Ru_{mean}, $Ru_{33\%}$, $Ru_{10\%}$, $Ru_{2\%}$ and Ru_{max} were evaluated. The observed wave run-up elevation time series was recorded by a beach camera system along the cross transect evidenced in Fig. 1b on February 10th 2016 from 08:00am to 16:00pm.

Run-up video records (Figs. 10 and 11) were made using the central camera of the video monitoring system described in section 3.4.

Table 2 show the statistical measures used to describe the skill of the different run-up formulas. The comparison between the hourly mean of the observed and simulated $Ru_{2\%}$ is reported in Fig. 12. A first visual analysis shows that the simulated $Ru_{2\%}$ is almost always underestimated with respect to the observed one. In detail, the Holman (1986) equation gives the best matching with the observed values, with a mean RMSE of 0.41m, the Mase (1989) equation gives a slightly worse matching, with a mean RMSE of 0.70m, and Stockdon et al. (2006) equation gives the worst results with a mean RMSE of 0.95m. Conversely, the SPS values are in decreasing order, that is 0.92, 0.87 and 0.83, respectively. Fig. 13 shows the comparison between hourly mean of observed and simulated run-up levels $Ru_{x\%}$ obtained by Mase (1989) equation. The results show a more uniform results of the numerical simulations in the eight hours of analysis, due to the lower time resolution of the WW3 model. Moreover, the results confirm that the best agreement with the observations is obtained for Ru_{max}, followed by $Ru_{10\%}$ and $Ru_{33\%}$, while the agreement for Ru_{mean} and $Ru_{2\%}$ is lower. These qualitative results are confirmed by the statistical indices reported in table 3, which can be synthesized using the Summary Performance Score (Melby et al., 2012), an average of normalized RMSE, BI and SI with an 0-1 scale, where 1 means no error. The values of this index are 0.96 for Ru_{max}, 0.95 for $Ru_{10\%}$ and 0.90 $Ru_{33\%}$, while it is 0.87 for $Ru_{2\%}$ and 0.75 for Ru_{mean}.

Table 2. $Ru_{x\%}$ observed with cameras versus $Ru_{x\%}$ simulated using different equations.

	Simulated run-up							Observed run-up				
	Holman (1986)	Mase (1989)					Stockdon (2006)					
	$Ru_{2\%}$	$Ru_{2\%}$	$Ru_{10\%}$	$Ru_{33\%}$	Ru_{max}	Ru_{mean}	$Ru_{2\%}$	Ru_{mean}	Ru_{max}	$R_{2\%}$	$R_{10\%}$	$R_{33\%}$
10/02 08-09	3.74	3.46	3.16	2.57	4.22	1.65	3.14	1.80	4.44	3.92	3.05	2.04
10/02 09-10	3.81	3.52	3.21	2.62	4.30	1.67	3.21	1.82	3.98	3.63	3.31	2.07
10/02 10-11	3.88	3.58	3.27	2.66	4.38	1.70	3.28	2.13	4.50	4.36	3.43	2.24
10/02 11-12	3.85	3.53	3.23	2.63	4.33	1.68	3.26	2.27	4.42	4.10	3.42	2.56
10/02 12-13	3.84	3.49	3.19	2.60	4.29	1.66	3.26	2.48	4.12	3.95	3.45	2.63
10/02 13-14	3.85	3.48	3.18	2.59	4.28	1.66	3.27	2.54	4.55	4.33	3.57	2.71
10/02 14-15	4.00	3.63	3.32	2.70	4.46	1.73	3.40	2.62	4.75	4.52	3.44	2.80
10/02 15-16	4.11	3.76	3.44	2.80	4.62	1.79	3.50	2.86	5.00	4.80	3.62	2.94

Table 3. Statistical error parameters obtained from the comparison between observed and simulated wave run-up levels.

	R	BI	SI	RMSE	NRMSE	$NRMSE_P$	BI_P	SI_P	SPS
Holman (1986) $Ru_{2\%}$	0.867	-0.075	0.062	0.410	0.097	0.903	0.925	0.938	0.972
Mase (1989) Ru_{mean}	0.424	-0.274	0.157	0.723	0.309	0.691	0.726	0.843	0.753
Mase (1989) $Ru_{33\%}$	0.607	0.059	0.112	0.318	0.126	0.874	0.941	0.888	0.901
Mase (1989) $Ru_{10\%}$	0.576	-0.047	0.039	0.209	0.061	0.939	0.953	0.961	0.951
Mase (1989) $Ru_{2\%}$	0.794	-0.154	0.067	0.704	0.167	0.833	0.846	0.933	0.871
Mase (1989) Ru_{max}	0.763	-0.025	0.051	0.255	0.057	0.943	0.975	0.949	0.956
Stockdon (2006) $Ru_{2\%}$	0.871	-0.217	0.063	0.949	0.225	0.	0.783	0.775	0.832

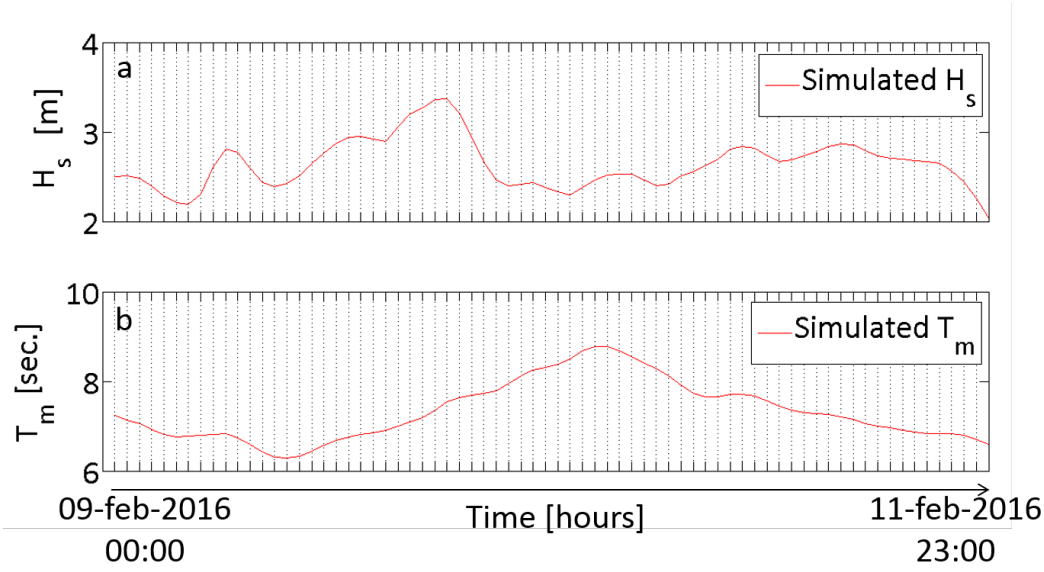

Figure 9. Forecasted significant wave height (H_s) and mean wave period (T_m) relative February 09th-11th 2016 sea storm at virtual buoy near Bonassola beach.

5 Discussion

The validation results of the offshore wave simulations and of the run-up calculations by means of observations techniques are here discussed.

The comparison between the simulated waves in offshore conditions and the altimeter data showed a satisfactory agreement with a BIAS of 0.192 and a standard deviation (SD) lower than 0.6. These results are the same order of magnitude of Wahle et al. (2017) who obtained a BIAS of -0.29 and SD of 1.07. The validation results of the $Ru_{2\%}$ formulas accuracy was done in terms of their RMSE and SPS. The most accurate formula was the one by Holman (1986) (RMSE=0.41), followed by Mase (1989) (RMSE=0.70) and by Stockdon et al. (2006) (RMSE=0.95).

In terms of SPS, the results of the run-up simulations obtained with Holman (1986) equation closely follow the video camera observations (SPS=0.97), with a good agreement with those of Melby et al. (2012) (SPS=0.84). The other formulations, for which the SPS value is similar to Holman's one, give satisfactory results too (SPS=0.87 for Mase (1989), SPS=0.83 for Stockdon et al. (2006)).

The under-prediction of the run-up levels by the Stockdon et al. (2006) equation has already been noted and explained by Poate et al. (2016) who analyzed video derived run-up statistics in six field sites collected over a two year period under energetic storm conditions on gravel beaches. They concluded that the Stockdon et al. (2006) equation under-predicts run-up $Ru_{2\%}$ levels on gravel beaches under energetic conditions by over 50%. For these reasons, more research is needed for the acquisition of a more general equation, which can be valid for both sand and gravel beaches.

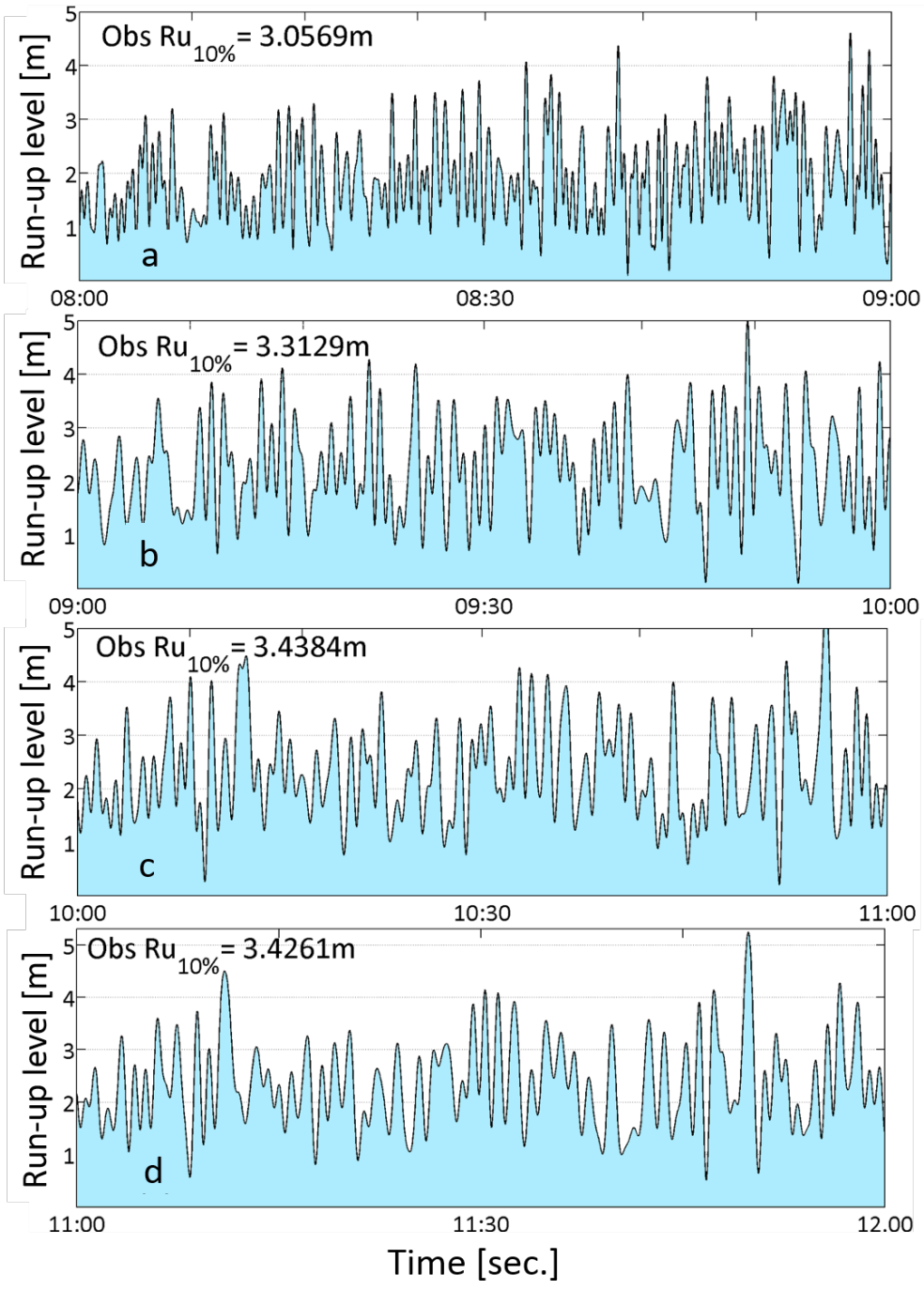

Figure 10. Wave run-up levels collected using pixel time stacks derived from video data of camera at Bonassola on February 10th 2016 at: (a) 8:00-9:00 UTC; (b) 9:00-10:00 UTC; (c) 10:00-11:00 UTC; (d) 11:00-12:00 UTC

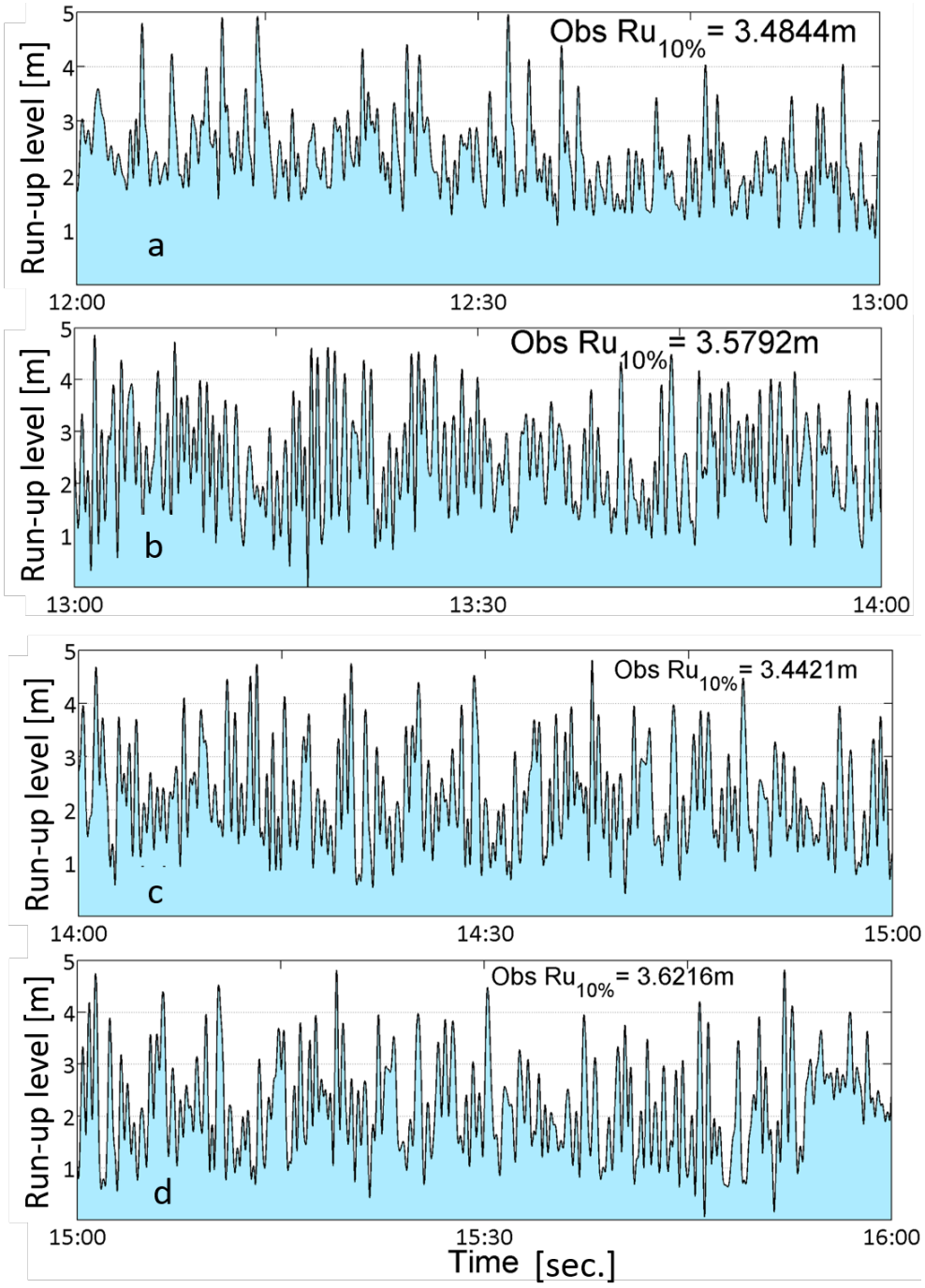

Figure 11. Wave run-up levels collected using pixel time stacks derived from video data of camera at Bonassola on February 10th 2016 at: (a) 12:00-13:00 UTC; (b) 13:00-14:00 UTC; (c) 14:00-15:00 UTC; (d) 15:00-16:00 UTC.

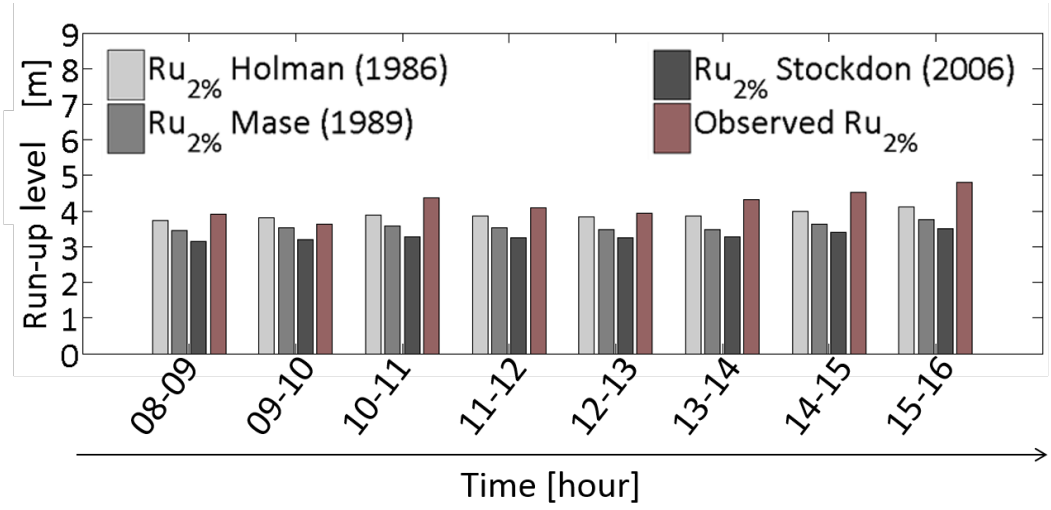

Figure 12. Comparison among observed and simulated $Ru_{2\%}$ with different formulas.

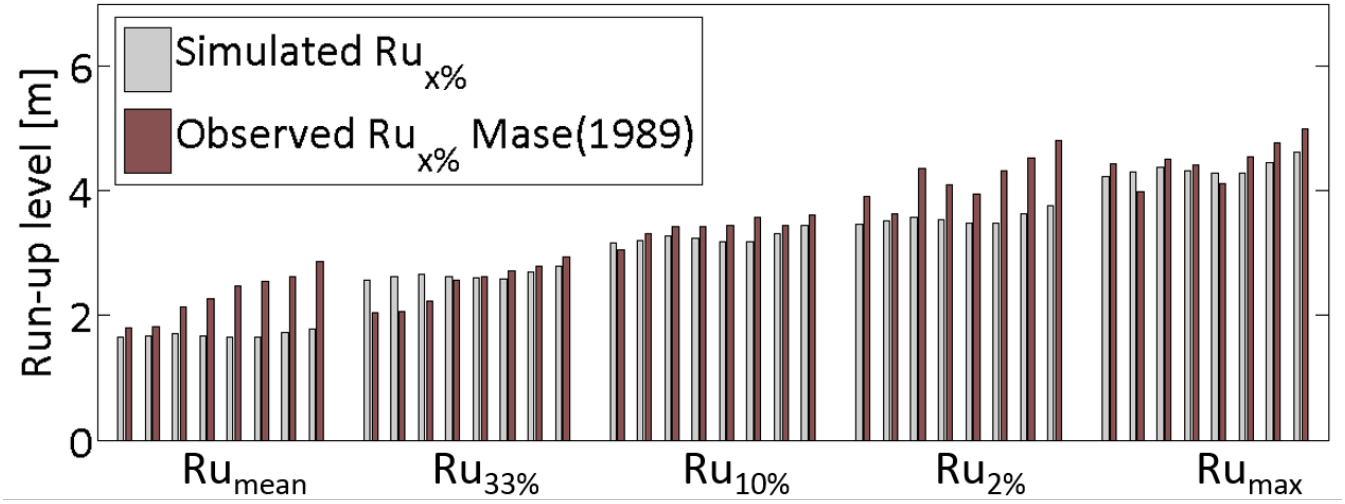

Figure 13. Comparison among different $Ru_{x\%}$ calculated with Mase (1989) equations and observations.

6 Conclusion and future directions

We configured a community and ad-hoc developed numerical model chain which starts from the forecasted wind till offshore wave and beach run-up simulations. The proposed model chain was tested by satellite altimeter data and video recorded images.

The comparison between the simulated and observed results in the swash zone shows that the wind-wave modelling chain gives

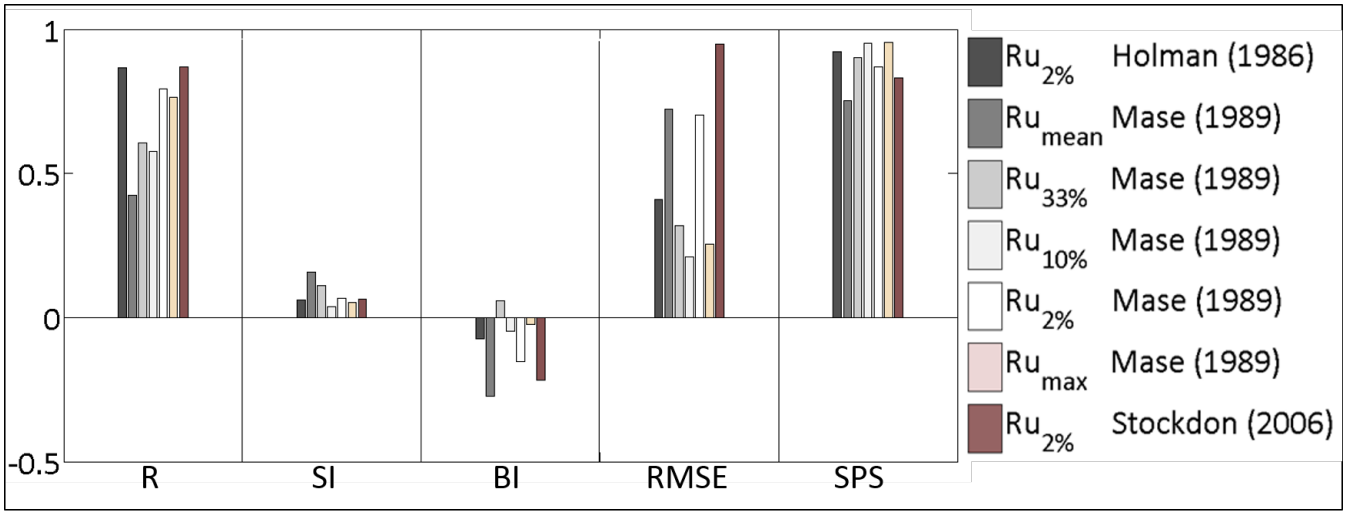

Figure 14. Bar diagram of statistical error parameters reported in Table 3.

also reliable results for simulations of the beach inundation in the time domain.

However, the run-up equations, which are used for coastal vulnerability studies have to be used with caution, particularly on gravel beaches. This considerations stimulate us to extend the field campaign to other beaches with different sediment characteristics and to test the equations in the coastal vulnerability and risk evaluation context.

In the near future, we will increase the spatial and temporal resolution of the WW3 model in order to enable the run-up calculations for more complex beach configurations. This improvement will need the implementation of the model chain using a cloud computing powered (Montella et al., 2015) GPGPU based approach (Di Lauro et al., 2012) in order to reduce the overall computational costs.

Acknowledgements. The authors are grateful to the CCMMMA (*Campania Center for Marine and Atmospheric Monitoring and Modelling*, http://meteo.uniparthenope.it), that is the forecast service of the University of Napoli "*Parthenope*" for the real time monitoring and forecast of marine, weather and air quality conditions in the Mediterranean area. The CCMMMA provided the hardware and software resources for the offshore numerical simulations.

References

Aagaard, T. and Holm, J.: Digitization of wave run-up using video records, Journal of Coastal Research, pp. 547–551, 1989.

Airy, G. B.: Tides and waves, Encyclopaedia Metropolitana, 3, 1817–1845, 1841.

Ascione, I., Giunta, G., Mariani, P., Montella, R., and Riccio, A.: A grid computing based virtual laboratory for environmental simulations, Euro-Par 2006 Parallel Processing, pp. 1085–1094, 2006.

Aucelli, P. P. C., Di Paola, G., Incontri, P., Rizzo, A., Vilardo, G., Benassai, G., Buonocore, B., and Pappone, G.: Coastal inundation risk assessment due to subsidence and sea level rise in a Mediterranean alluvial plain (Volturno coastal plain–southern Italy), Estuarine, Coastal and Shelf Science, 2016.

Battjes, J. A.: Surf similarity, in: Coastal Engineering, Proceedings of 14th Conference on Coastal Engineering, Copenhagen, Denmark, 1974, vol. 14, pp. 466–480, ASCE, 1975.

Battjes, J. A. and Janssen, J.: Energy loss and set-up due to breaking of random waves, in: Coastal Engineering 1978, pp. 569–587, 1978.

Benassai, G. and Ascione, I.: Implementation and validation of wave watch III model offshore the coastlines of Southern Italy, in: Proceedings of 25th International Conference on Offshore Mechanics and Arctic Engineering, pp. 553–560, American Society of Mechanical Engineers, 2006a.

Benassai, G. and Ascione, I.: Implementation of WWIII wave model for the study of risk inundation on the coastlines of Campania, Italy, Environmental Problems in Coastal Regions VI: Including Oil Spill Studies, 88, 249, 2006b.

Benassai, G., Migliaccio, M., Montuori, A., and Ricchi, A.: Wave Simulations Through Sar Cosmo-Skymed Wind Retrieval and Verification with Buoy Data, in: Proceedings of the Twenty-second International Offshore and Polar Engineering Conference, International Society of Offshore and Polar Engineers, 2012.

Benassai, G., Migliaccio, M., and Montuori, A.: Sea wave numerical simulations with COSMO-SkyMed© SAR data, Journal of Coastal Research, 65, 660–665, 2013a.

Benassai, G., Montuori, A., Migliaccio, M., and Nunziata, F.: Sea wave modeling with X-band COSMO-SkyMed© SAR-derived wind field forcing and applications in coastal vulnerability assessment, Ocean Science, 9, 325, 2013b.

Benassai, G., Di Paola, G., and Aucelli, P. P. C.: Coastal risk assessment of a micro-tidal littoral plain in response to sea level rise, Ocean & Coastal Management, 104, 22–35, 2015a.

Benassai, G., Migliaccio, M., and Nunziata, F.: The use of COSMO-SkyMed© SAR data for coastal management, Journal of Marine Science and Technology, 20, 542–550, 2015b.

Benassai, G., Aucelli, P., Budillon, G., De Stefano, M., Di Luccio, D., Di Paola, G., Montella, R., Mucerino, L., Sica, M., and Pennetta, M.: Rip current evidence by hydrodynamic simulations, bathymetric surveys and UAV observation, Natural Hazards and Earth System Sciences, 17, 1493–1503, 2017.

Bertotti, L. and Cavaleri, L.: Wind and wave predictions in the Adriatic Sea, Journal of Marine Systems, 78, S227–S234, 2009.

Bidlot, J.-R., Holmes, D. J., Wittmann, P. A., Lalbeharry, R., and Chen, H. S.: Intercomparison of the performance of operational ocean wave forecasting systems with buoy data, Weather and Forecasting, 17, 287–310, 2002.

Brignone, M., Schiaffino, C. F., Isla, F. I., and Ferrari, M.: A system for beach video-monitoring: Beachkeeper plus, Computers & Geosciences, 49, 53–61, 2012.

Carratelli, E. P., Budillon, G., Dentale, F., Napoli, F., Reale, F., and Spulsi, G.: An experience in monitoring and integrating wind and wave data in the Campania Region, Bollettino di Geofisica Teorica ed Applicata, 48, 215–226, 2007.

Casella, E., Rovere, A., Pedroncini, A., Mucerino, L., Casella, M., Cusati, L. A., Vacchi, M., Ferrari, M., and Firpo, M.: Study of wave runup using numerical models and low-altitude aerial photogrammetry: A tool for coastal management, Estuarine, Coastal and Shelf Science, 149, 160–167, 2014.

Cavaleri, L. and Rizzoli, P. M.: Wind wave prediction in shallow water: Theory and applications, Journal of Geophysical Research: Oceans, 86, 10 961–10 973, 1981.

Di Lauro, R., Giannone, F., Ambrosio, L., and Montella, R.: Virtualizing general purpose GPUs for high performance cloud computing: an application to a fluid simulator, in: Parallel and Distributed Processing with Applications (ISPA), 2012 IEEE 10th International Symposium on, pp. 863–864, IEEE, 2012.

Di Paola, G., Aucelli, P. P. C., Benassai, G., and Rodríguez, G.: Coastal vulnerability to wave storms of Sele littoral plain (southern Italy), Natural hazards, 71, 1795–1819, 2014.

Didenkulova, I.: Marine natural hazards in coastal zone: observations, analysis and modelling (Plinius Medal Lecture), in: EGU General Assembly Conference Abstracts, vol. 12, p. 14748, 2010.

Didenkulova, I. and Pelinovsky, E.: Run-up of long waves on a beach: the influence of the incident wave form, Oceanology, 48, 1–6, 2008.

Didenkulova, I., Sergeeva, A., Pelinovsky, E., and Gurbatov, S.: Statistical estimates of characteristics of long-wave run-up on a beach, Izvestiya, Atmospheric and Oceanic Physics, 46, 530–532, 2010.

Dodd, N.: Numerical model of wave run-up, overtopping, and regeneration, Journal of Waterway, Port, Coastal, and Ocean Engineering, 124, 73–81, 1998.

Fenton, J. D. and McKee, W.: On calculating the lengths of water waves, Coastal Engineering, 14, 499–513, 1990.

Goda, Y.: On the methodology of selecting design wave height, in: Coastal Engineering Proceedings 1988, vol. 21, pp. 899–913, ASCE, 1989.

Hasselmann, K.: Measurements of wind wave growth and swell decay during the Joint North Sea Wave Project (JONSWAP), Dtsch. Hydrogr. Z., 8, 95, 1973.

Hasselmann, S. and Hasselmann, K.: Computations and parameterizations of the nonlinear energy transfer in a gravity-wave spectrum. Part I: A new method for efficient computations of the exact nonlinear transfer integral, Journal of Physical Oceanography, 15, 1369–1377, 1985.

Holland, K. T. and Holman, R. A.: Video estimation of foreshore topography using trinocular stereo, Journal of Coastal Research, pp. 81–87, 1997.

Holman, R.: Extreme value statistics for wave run-up on a natural beach, Coastal Engineering, 9, 527–544, 1986.

Hubbard, M. E. and Dodd, N.: A 2D numerical model of wave run-up and overtopping, Coastal Engineering, 47, 1–26, 2002.

Hunt, I. A.: Design of sea-walls and breakwaters, Transactions of the American Society of Civil Engineers, 126, 542–570, 1959.

Jennings, R. and Shulmeister, J.: A field based classification scheme for gravel beaches, Marine Geology, 186, 211–228, 2002.

Johannessen, O. and Bjorgo, E.: Wind energy mapping of coastal zones by synthetic aperture radar (SAR) for siting potential windmill locations, International Journal of Remote Sensing, 21, 1781–1786, 2000.

Leonard, B. P.: A stable and accurate convective modelling procedure based on quadratic upstream interpolation, Computer methods in applied mechanics and engineering, 19, 59–98, 1979.

Mase, H.: Random wave runup height on gentle slope, Journal of Waterway, Port, Coastal, and Ocean Engineering, 115, 649–661, 1989.

Melby, J., Caraballo-Nadal, N., and Kobayashi, N.: Wave runup prediction for flood mapping, Coastal Engineering Proceedings, 1, 79, 2012.

Mentaschi, L., Besio, G., Cassola, F., and Mazzino, A.: Developing and validating a forecast/hindcast system for the Mediterranean Sea, Journal of Coastal Research, 65, 1551–1556, 2013.

Montella, R., Giunta, G., and Riccio, A.: Using grid computing based components in on demand environmental data delivery, in: Proceedings of the second workshop on Use of P2P, GRID and agents for the development of content networks, pp. 81–86, ACM, 2007.

Montella, R., Agrillo, G., Mastrangelo, D., and Menna, M.: A globus toolkit 4 based instrument service for environmental data acquisition and distribution, in: Proceedings of the third international workshop on Use of P2P, grid and agents for the development of content networks, pp. 21–28, ACM, 2008.

Montella, R., Giunta, G., Laccetti, G., Lapegna, M., Palmieri, C., Ferraro, C., and Pelliccia, V.: Virtualizing CUDA Enabled GPGPUs on ARM Clusters., in: PPAM (2), pp. 3–14, 2015.

Montuori, A., Ricchi, A., Benassai, G., and Migliaccio, M.: Sea Wave Numerical Simulation and Verification in Tyrrhenian Costal area with X-Band COSMO-Skymed SAR data, in: Proceedings of the ESA, SOLAS & EGU Joint Conference Earth Observation for Ocean-Atmosphere Interactions Science, ESA-ESRIN, Frascati, Italy, vol. 703, ESA-SP, 2011.

Nunziata, F., Buono, A., Migliaccio, M., and Benassai, G.: Dual-polarimetric C-and X-band SAR data for coastline extraction, IEEE Journal of Selected Topics in Applied Earth Observations and Remote Sensing, 9, 4921–4928, 2016.

Ojeda, E., Ruessink, B., and Guillen, J.: Morphodynamic response of a two-barred beach to a shoreface nourishment, Coastal Engineering, 55, 1185–1196, 2008.

Pham, Q., Malik, T., Foster, I. T., Di Lauro, R., and Montella, R.: SOLE: Linking Research Papers with Science Objects., in: IPAW, pp. 203–208, Springer, 2012.

Poate, T. G., McCall, R. T., and Masselink, G.: A new parameterisation for runup on gravel beaches, Coastal Engineering, 117, 176–190, 2016.

Reale, F., Dentale, F., Carratelli, E. P., and Torrisi, L.: Remote sensing of small-scale storm variations in coastal seas, Journal of Coastal Research, 30, 130–141, 2014.

Rusu, L., Bernardino, M., and Guedes Soares, C.: Wind and wave modelling in the Black Sea, Journal of Operational Oceanography, 7, 5–20, 2014.

Shore Protection Manual, .: Department of the Army, Waterways Experiment Station, Corps of Engineers, Coastal Engineering Researcher Center, 2, 1984.

Skamarock, W. C., Klemp, J. B., and Dudhia, J.: Prototypes for the WRF (Weather Research and Forecasting) model, in: Preprints, Ninth Conf. Mesoscale Processes, J11–J15, Amer. Meteorol. Soc., Fort Lauderdale, FL, 2001.

Stockdon, H. F., Holman, R. A., Howd, P. A., and Sallenger, A. H.: Empirical parameterization of setup, swash, and runup, Coastal engineering, 53, 573–588, 2006.

Takewaka, S. and Nakamura, T.: Surf zone imaging with a moored video system, in: Proceedings of the International Conference on Coastal Engineering 2000, pp. 1211–1216, ASCE, 2001.

Tolman, H. L.: Effects of numerics on the physics in a third-generation wind-wave model, Journal of physical Oceanography, 22, 1095–1111, 1992.

Tolman, H. L.: Alleviating the garden sprinkler effect in wind wave models, Ocean Modelling, 4, 269–289, 2002.

Tolman, H. L. and Chalikov, D.: Source terms in a third-generation wind wave model, Journal of Physical Oceanography, 26, 2497–2518, 1996.

Tolman, H. L. et al.: User manual and system documentation of WAVEWATCH III TM version 3.14, Technical note, MMAB Contribution, 276, 220, 2009.

van der Meer, J., Allsop, N., Bruce, T., De Rouck, J., Kortenhaus, A., Pullen, T., Schüttrumpf, H., Troch, P., and Zanuttigh, B.: EurOtop: Manual on wave overtopping of sea defences and related sturctures-An overtopping manual largely based on European research, but for worlwide application, 2016.

Wahle, K., Staneva, J., Koch, W., Fenoglio-Marc, L., Ho-Hagemann, H. T., and Stanev, E. V.: An atmosphere–wave regional coupled model: improving predictions of wave heights and surface winds in the southern North Sea, Ocean Science, 13, 289, 2017.

Zhang, S. and Zhang, C.: Application of ridgelet transform to wave direction estimation, in: Image and Signal Processing, 2008. CISP'08. Congress on, vol. 2, pp. 690–693, IEEE, 2008.